Journal of Systemics, Cybernetics and Informatics (2021) 19(8), 164-181
https://doi.org/10.54808/JSCI.19.08.164

How Does a Cell Change Flow Direction Due to a Micro Groove?

[*]Shigehiro Hashimoto[1] Taketo Matsumoto[1] and Shogo Uehara[1]

[1] *Kogakuin University*

Abstract[1]

The change in direction of a cell flowing over an oblique micro groove has been analyzed in vitro. The micro flow-channel (0.05 mm height × 1 mm width × 25 mm length) with oblique micro grooves (4.5 μm depth) was manufactured on a polydimethylsiloxane (PDMS) disk by the micromachining technique. The angle between the main flow direction and the longitudinal axis of the groove is 45 degrees. The effect of variation of the groove width (0.03 mm, 0.04 mm, and 0.05 mm) was studied. Myoblasts (C2C12: mouse myoblast cell line) were used in the test. The main flow velocity (0.02 mm/s < vx < 0.23 mm/s) of the medium was controlled by the pressure difference between the inlet and the outlet. The shape of each flowing cell was tracked on a movie recorded by the camera attached to the eyepiece of the microscope. The experimental results show that the change of the direction of each cell by each groove depends on the shape of the cell, which depends on both the shape of the cell and the width of the groove.

Keywords: *Biomedical Engineering, C2C12, Micro Groove, Micro Flow Channel and Shape index.*

1. Introduction

The technology of sorting of cells can be applied to regenerative medicine to select the target cells (Sivaramakrishnan, 2020). It also can be applied to diagnostics to handle the target cell (Yoon, 2019).

Several methods were proposed for the sorting of biological cells *in vitro*. The minimally invasive method is preferable. The microfluidic systems were used in some methods. In these systems, a variety of properties of cells were used for the sorting: electric fields (Hashimoto, 2020), magnetic fields, dimension, density or deformability (Zhang, 2019). In the present study, physical properties of the single flowing cell have been analyzed: the shape, and deformation.

* Shigehiro Hashimoto, Mechanical Engineering, Kogakuin University, Tokyo, 192-0015, Japan (at13351@g.kogakuin.jp). This article was presented at WMSCI2021 in July 2021.
[1] The authors are grateful to Prof. Richard Magin for his proofreading of this article.

To capture the target cell, several kinds of morphology were designed in the microfluidic systems: electrodes (Hashimoto, 2020), micro slits (Takahashi, 2016) (Takahashi, 2017), micro holes (Hashimoto, 2014), or micro grooves (Takahashi, 2016). The photolithography technique enables manufacturing the micro-topography (Carlsen, 2020). The movement of each cell can change at the groove on the bottom wall of the flow channel (Hashimoto, 2019).

In the present study, the movement of a single cell flowing over the micro groove, which is manufactured by the photolithography technique, was analyzed *in vitro*.

2. Methods

2.1. Flow Channel with Micro Grooves on Bottom

For changing the movement of each flowing cell, three micro grooves of rectangular shapes (the depth of 4.5 μm depth, and 0.2 mm length) have been fabricated on the surface of the polydimethylsiloxane (PDMS) plate with the photolithography technique (Hashimoto, 2019). The grooves are arranged on the bottom of the micro flow channel. The angle between the main flow direction and the longitudinal axis of the groove is 45 degrees. As to the serial groove arrangement from upstream to downstream, variation has been made on the width (w) of the groove: 0.03 mm, 0.04 mm, and 0.05 mm (Figure 1).

Both the upper and the lower PDMS plates were exposed to the oxygen gas (0.1 Pa, 30 cm^3/min) in the reactive ion etching system (FA-1) (oxygen plasma ashing, 50 W, for thirty seconds). Immediately after ashing, the upper disk adheres (plasma bonding) to the lower disk to make the flow path (0.05 mm height × 1 mm width × 25 mm length) between them. The flow channel is placed on the stage of the inverted phase-contrast microscope (IX71, Olympus Co., Ltd., Tokyo).

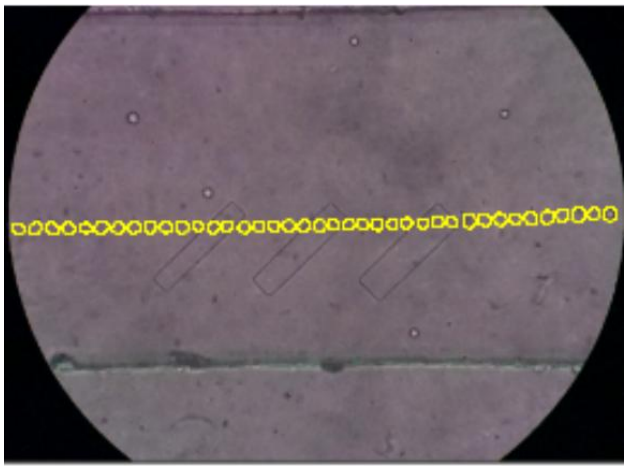

Figure 1: Trace of cell (No. 1) flowing (from left to right) over three grooves.

2.2. Cell Flow Test

C2C12 (passage < 10, mouse myoblast cell line originated with cross-striated muscle of C3H mouse) was used in the test. Cells were pre-cultured with the D-MEM (Dulbecco's Modified Eagle's Medium) containing 10% FBS and 1% of Antibiotic-Antimycotic (penicillin, streptomycin and amphotericin B, Life Technologies) in the incubator for one week.

The inner surface of the flow channel was hydrophilized by the oxygen (30 cm^3/min, 0.1 Pa) plasma ashing for one minute at 100 W by the reactive ion etching system (FA-1), and prefilled with the bovine serum albumin solution for thirty minutes at 310 K.

Just before the flow test, the cells were exfoliated from the plate of the culture dish with trypsin, and suspended in the D-MEM (Dulbecco's Modified Eagle's Medium). The suspension of cells (0.06 cm^3; 4000 cells/cm^3) was poured at the inlet of the flow channel. The flow (the main flow velocity (0.02 mm/s < v_x < 0.23 mm/s)) occurs by the pressure difference between the inlet and the outlet. The small reservoir (the depth of 3 mm and the diameter of 5 mm) at the inlet makes the pressure head. Each

cell rolling over the micro grooves was observed by the microscope, and recorded by the camera (DSC-RX100M4, Sony Corporation, Japan), which is set on the eyepiece of the microscope.

2.3. Analysis of Flowing Cell Shape

" Image J" was applied to analyze the behavior of each cell. On the microscopic image, the outline of each cell was traced. The two-dimensional projected area S of each cell was measured. The area S of the tracked cell varies in the groove. The change of the area in each groove was calculated as ΔS. The ratio of the area change was calculated as $\Delta S/Smax$, where $Smax$ is the maximum value of S in the groove for the tracked cell. The value of $\Delta S/Smax$ is 0.5, when the area S of the cell is doubled in the groove. The contour of each cell was approximated to ellipse (Figure 2). The centroid was traced to track the movement of the cell. The coordinate was defined as follows: the direction of flow is x, and the direction perpendicular to the flow is y (Figure 2). On the ellipse, the length of the major axis (a), and the length of the minor axis (b) were measured. The ratio of axes is calculated as the shape index (P) by Equation (1).

$$P = 1 - b / a \tag{1}$$

Clearly, $P = 0$ for a circle, and as the shape of the ellipse narrows, $a >> b$, such that P approaches to 1. The absolute value of the shape index change in each groove was calculated as ΔP.

The angle (-90 degrees $< \theta <$ 90 degrees) between the direction of the main flow of the medium and the direction of the major axis of each cell was measured for the microscopic image. When the major axis is parallel to the direction of the flow, $\theta = 0$. When the major axis is perpendicular to the direction of the flow, $\theta = -90$ degrees or 90 degrees. The direction change of the major axis of the cell at each groove was measured as the acute angle (0 degrees $< \Delta\theta <$ 90 degrees).

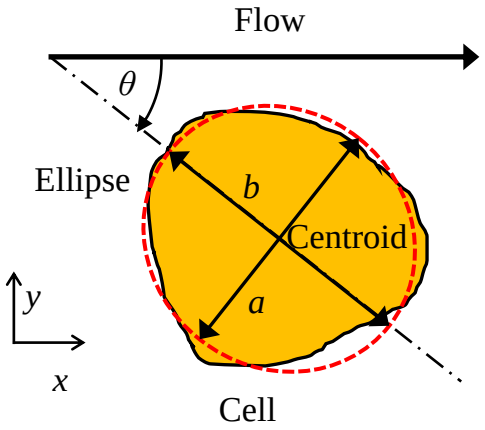

Figure 2: Parameters to analyze image of each single cell: contour is approximated to ellipse (major axis *a*, and minor axis *b*), angle (θ) between major axis (*a*) and flow direction (*x*).

3. Results

The tracing of the contour of each cell is exemplified in Figure 2. The tracking of the shape index (*P*) of each cell is illustrated in Figures 3a, 4a, and 5a, respectively. The tracking of the angle of the major axis of each cell is shown in Figures 3b, 4b, and 5b, respectively. The direction change of the major axis of the cell at each groove was measured as $\Delta\theta$ (Figure 7). The tracking of the position of each cell is exemplified in in Figures 3c, 4c, and 5c, respectively. The stepwise movement of the cell in y direction at each groove was measured as Δy (Figure 8). Each movement of the cell at three grooves is illustrated in Figures 3 and 4. In Figures 3 and 4, data plot of square, rhombus, and triangle show the movement at each groove of the width: 0.03 mm, 0.04 mm, and 0.05 mm, respectively. Figure 5 shows the movement of the cell, which does not pass over three grooves. Both the shape index and the angle of the major axis fluctuate during the movement of the cell along the medium flow. The fluctuation range of the shape index of each cell is wider over grooves (< 0.3; Figures 3a and 4a) than over the flat surface (< 0.2; Figure 5a). Every cell changes the direction of the movement at the groove (Figures 3c and 4c). Both the shape index and the major axis direction of each cell also change at the groove (Figures 3a, 3b, 4a, 4b). In Figures 3c, 4c, and 5c, *y* coordinate of the tracking of each cell

shows slow increase, because the main flow direction tilts by 1.1 degrees in the image captured by the camera.

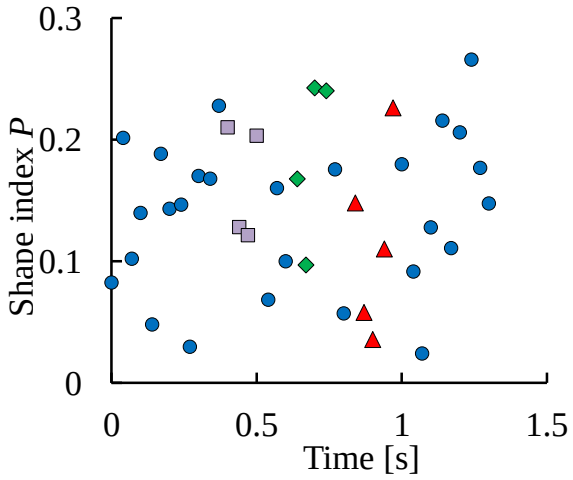

Figure 3a: Shape index (P) tracings: over groove of w = 0.03 mm (square), 0.04 mm (rhombus), 0.05 mm (triangle): (No. 1).

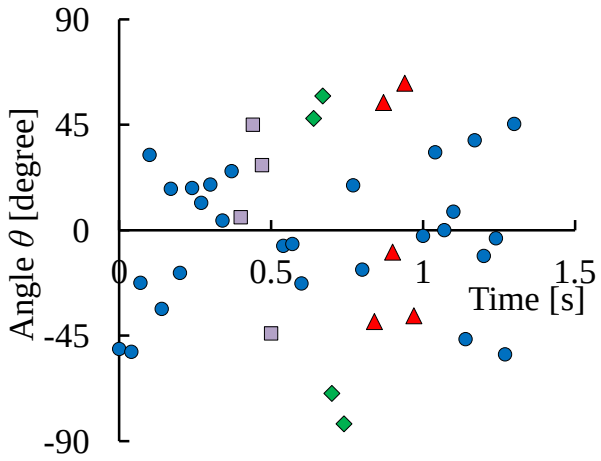

Figure 3b: Angle (θ) tracings: over groove of w = 0.03 mm (square), 0.04 mm (rhombus), 0.05 mm (triangle) (No. 1).

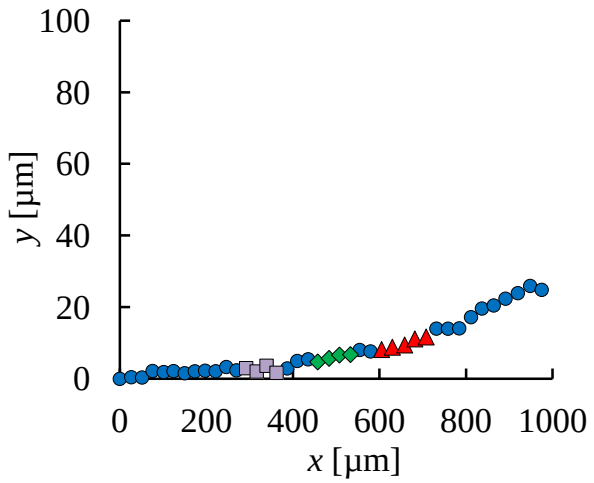

Figure 3c: Movement of cell: over groove of w = 0.03 mm (square), 0.04 mm (rhombus), 0.05 mm (triangle) (No. 1).

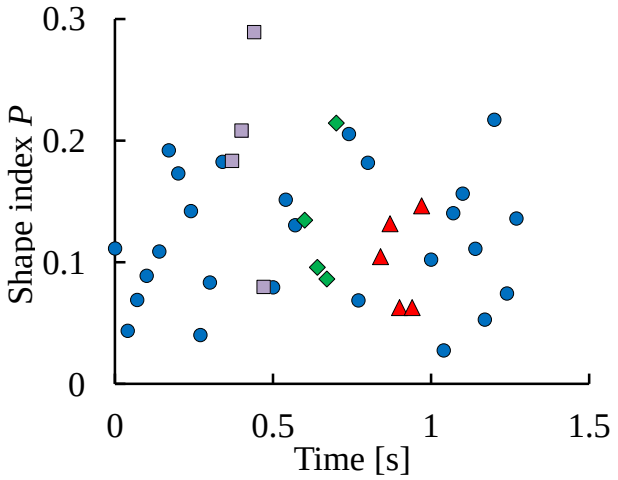

Figure 4a: Shape index (P) tracings: over groove of w = 0.03 mm (square), 0.04 mm (rhombus), 0.05 mm (triangle): (No. 2).

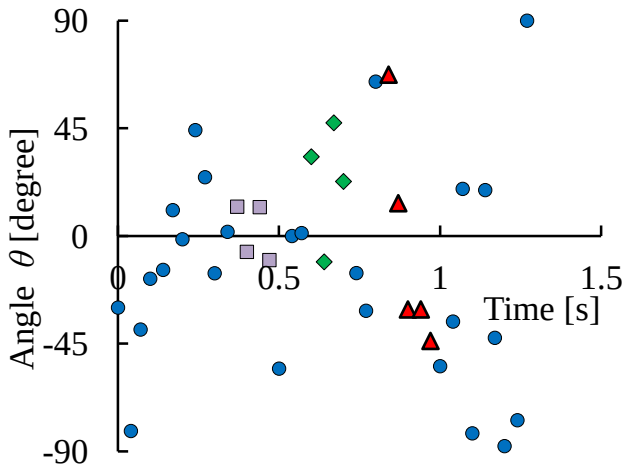

Figure 4b: Angle (θ) tracings: over groove of w = 0.03 mm (square), 0.04 mm (rhombus), 0.05 mm (triangle): (No. 2).

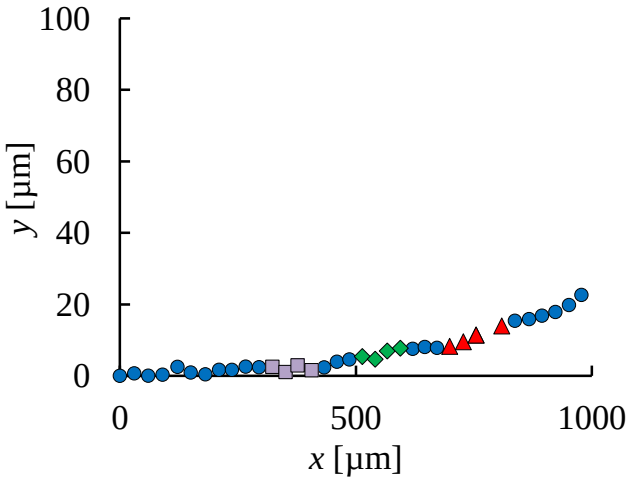

Figure 4c: Movement of cell: over groove of w = 0.03 mm (square), 0.04 mm (rhombus), 0.05 mm (triangle) (No. 2).

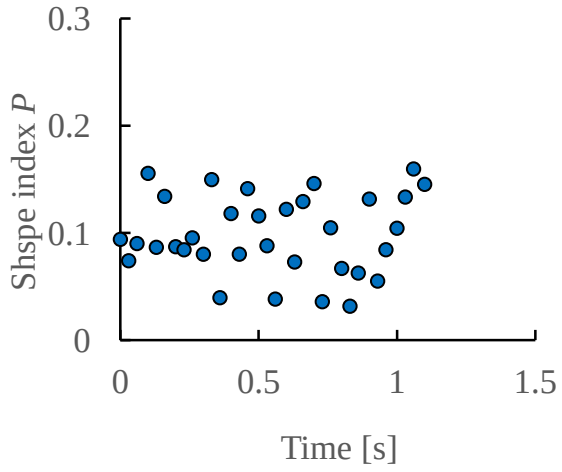

Figure 5a: Shape index tracings: control (No. 3).

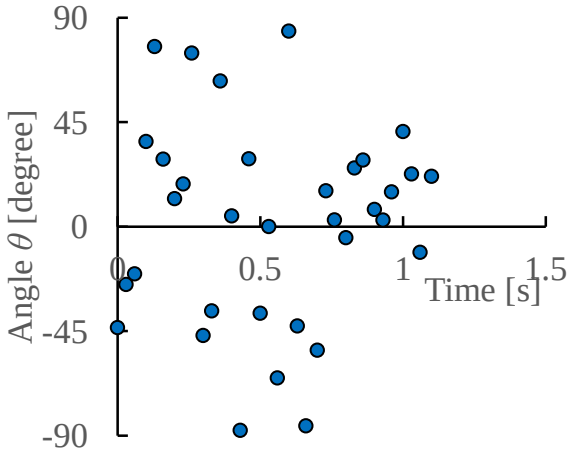

Figure 5b: Angle (θ) tracings: control (No. 3).

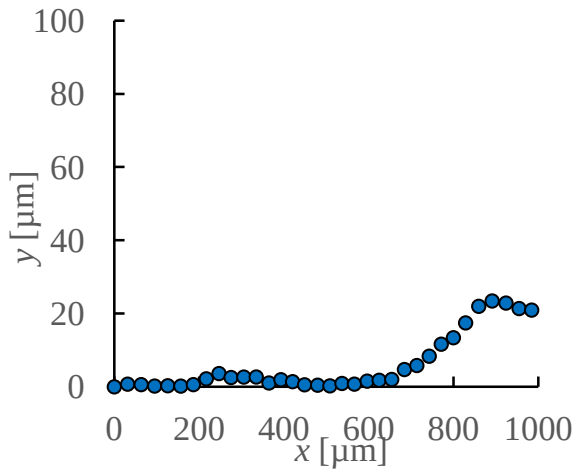

Figure 5c: Movement of cell: control (No. 3).

Figure 6 shows the relationship between the shape index change (ΔP) and the ratio of the area change ($\Delta S/Smax$). Figure 7 shows the relationship between the angle change ($\Delta\theta$) and the ratio of the area change ($\Delta S/Smax$). Figure 8 shows the relationship between y component of the stepwise movement of the cell (Δy) and the ratio of the area change ($\Delta S/Smax$). Figures 6a, 7a, and 8a show data at the groove of the width of 0.03 mm. Figures 6b, 7b, and 8b show data at the groove of the width of 0.04 mm. Figures 6c, 7c, and 8c show data at the groove of the width of 0.05 mm. The dotted line is the regression line of data in each figure (Figures 6-8). The correlation coefficient of data is calculated as r value in each figure.

The stepwise movement of the cell (Δy) is high around the ratio 0.3 of the area change ($\Delta S/Smax$) in every width of the groove (Figure 8). The shape index change (ΔP) decreases with the ratio of the area change ($\Delta S/Smax$) (Figure 6a) in the groove of 0.03 mm width. The angle change ($\Delta\theta$) increases with the ratio of the area change ($\Delta S/Smax$) (Figure 7a) in the groove of 0.03 mm width.

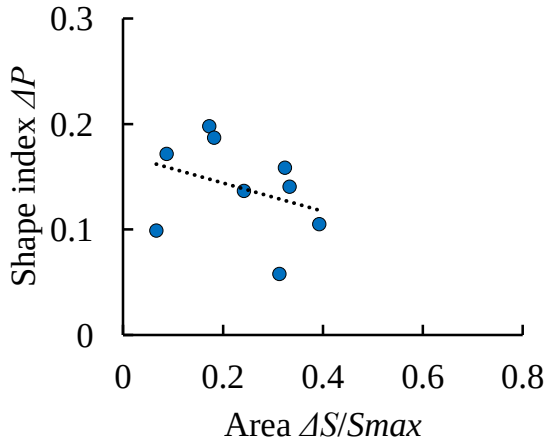

Figure 6a: Relationship between shape index (*ΔP*) and area (*ΔS*/*Smax*) over groove of 30 µm: dotted line, *ΔP* = − 0.13 (*ΔS*/*Smax*) + 0.17, *r* = 0.34.

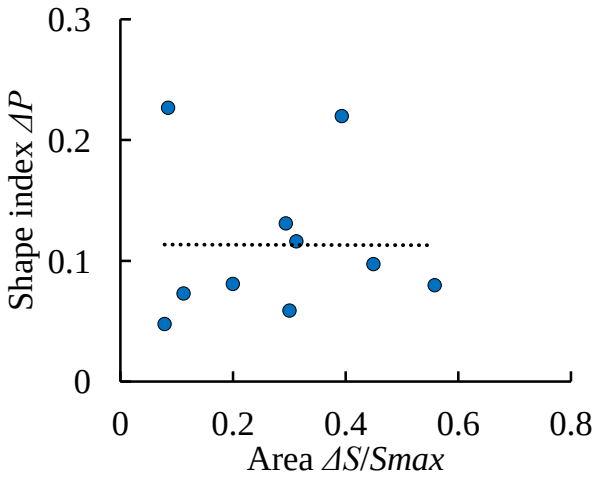

Figure 6b: Relationship between shape index (*ΔP*) and area (*ΔS*/*Smax*) over groove of 40 µm: dotted line, *ΔP* = − 0.0013 (*ΔS*/*Smax*) + 0.11, *r* = 0.003.

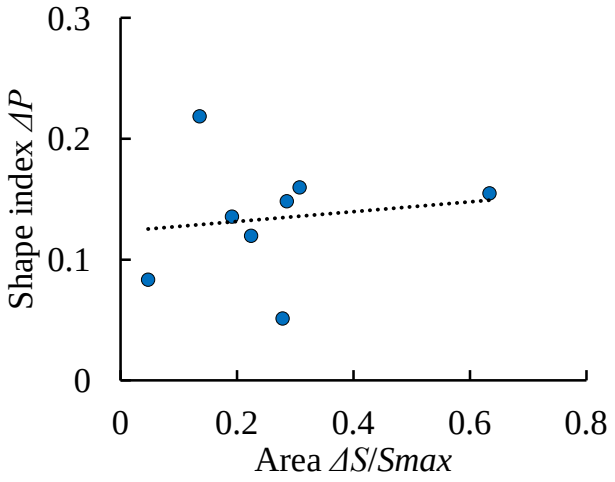

Figure 6c: Relationship between shape index (*ΔP*) and area (*ΔS*/*Smax*) over groove of 50 µm: dotted line, *ΔP* = 0.041 (*ΔS*/*Smax*) + 0.12, *r* = 0.14.

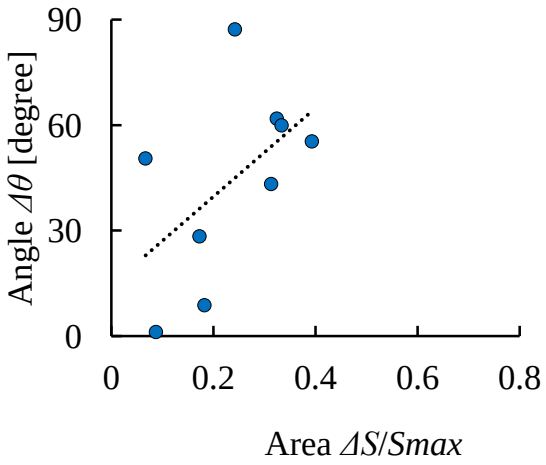

Figure 7a: Relationship between angle (*Δθ*) and area (*ΔS*/*Smax*) over groove of 30 µm: dotted line, *Δθ* = 126 (*ΔS*/*Smax*) + 15, *r* = 0.53.

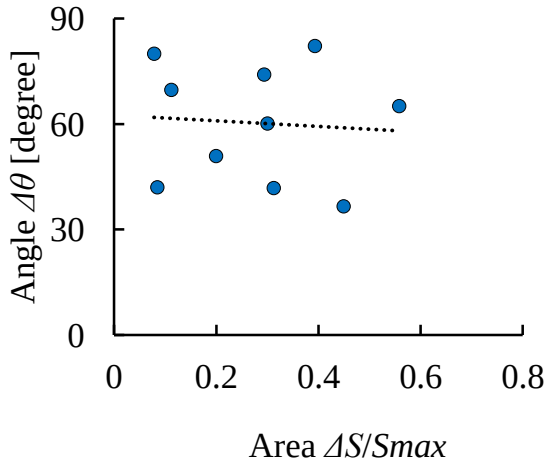

Figure 7b: Relationship between angle ($\Delta\theta$) and area ($\Delta S/Smax$) over groove of 40 µm: dotted line, $\Delta\theta = -7.9\ (\Delta S/Smax) + 62$, $r = 0.08$.

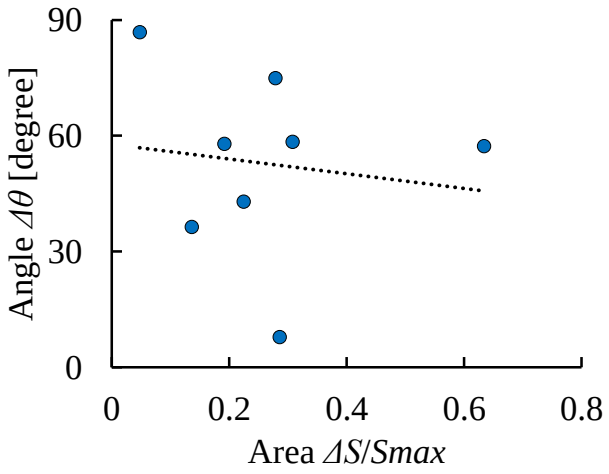

Figure 7c: Relationship between angle ($\Delta\theta$) and area ($\Delta S/Smax$) over groove of 50 µm: dotted line, $\Delta\theta = -19\ (\Delta S/Smax) + 58$, $r = 0.14$.

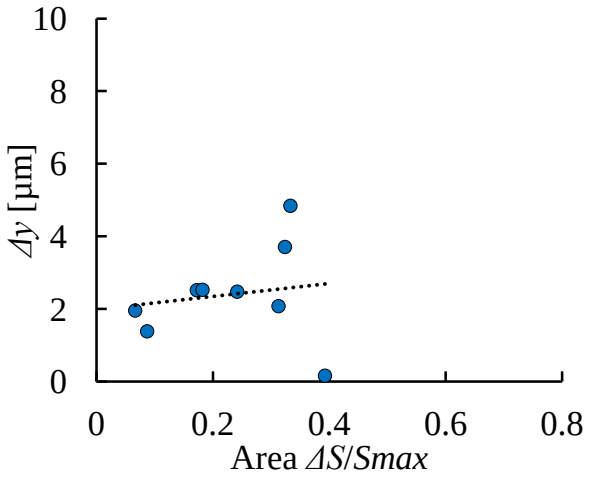

Figure 8a: Relationship between step (*Δy*) and area (*ΔS*/*Smax*) over groove of 30 µm: dotted line, *Δy* = 1.8 (*ΔS*/*Smax*) + 2, *r* = 0.16.

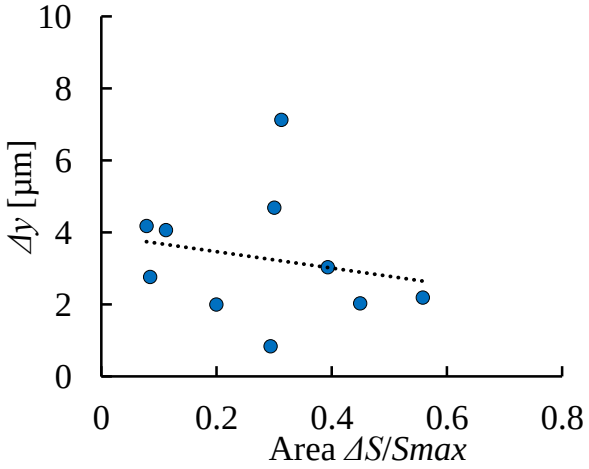

Figure 8b: Relationship between step (*Δy*) and area (*ΔS*/*Smax*) over groove of 40 µm: dotted line, *Δy* = − 2.3 (*ΔS*/*Smax*) + 3.9, *r* = 0.20.

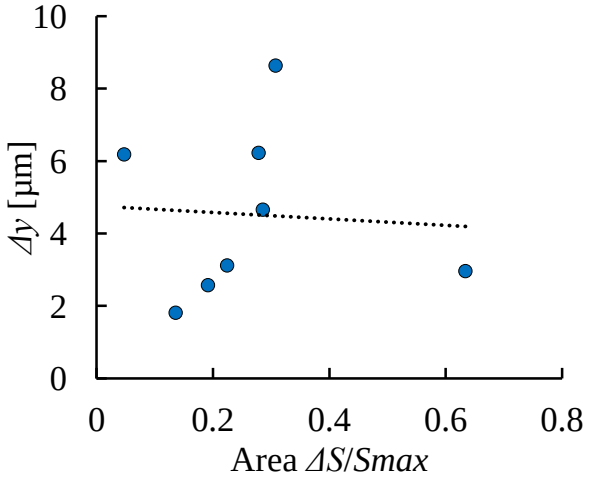

Figure 8c: Relationship between step (Δy) and area ($\Delta S/Smax$) over groove of 50 μm: dotted line, $\Delta y = -0.89\ (S/Smax) + 4.8$, $r = 0.07$.

4. Discussion

Filtration is one of the basic methods of cell sorting (LaBelle, 2021). Fluorescence techniques (Mutafopulos, 2019) were used in the previous sorting systems such as the flow cytometry technique. Non-destructive cell sorting systems, on the other hand, were designed in previous studies. The label-free methods were designed with microfluidic systems. Some of them were designed to capture cancer cells (Yoon, 2019).

Several fluid flow systems were used in the previous studies. For example, cylindrical and half-cylindrical (Hashimoto, 2014) holes were used for the trap of cells. The asymmetrical hole might be suitable for trap than the symmetrical hole. The rectangular grooves have been successfully manufactured on the wall of the micro fluid channel. The dimension of the grooves was confirmed by the laser microscope (Carlsen, 2020). The depths of the micro patterns were between 2 μm and 10 μm in the previous studies (Hashimoto, 2020). In the present study, the depth of the grooves is 4.5 μm, which is smaller than the diameter of the cells. The deeper hole may have the advantage to trap every cell. For the shallower trap, on the other hand, it is not easy to trap a cell. The trap of the appropriate dimension can distinguish cells. The duration of the trapped time of the cell might relate to

the interaction between the micro hole and the cell: the affinity between the cell and the surface of the micro pattern, or deformability of the cell.

The results of the previous study show that the movement of cell travelling on the wall is modified by the oblique micro groove on the wall under the cell velocity lower than 1 mm/s (Hashimoto, 2019). The angle of 45 degrees between the longitudinal direction of the groove and the flow direction is effective to shift the streamline of the cell. The stepwise movement along the oblique groove depends on the several parameters: the diameter of cells, the width of the groove, the velocity of the cell, and the shape of the cell (Hashimoto, 2019). As the diameter of the cell decreases, the traveling length along the groove increases. The movement may be related not only to the diameter but also to deformability of the cell. The movement of flowing cell at the bottom surface of the flow channel may be related to the specific gravity of the cell: the density difference between the cell and the medium. The shifted distance of malnourished cells by the oblique groove was smaller than that of normal cells in the previous study (Hashimoto, 2019). The shape of the cell can be detected by the movement of the flowing cell over the micro groove. In the previous study, the stepwise movement increased with the increase of the angle change at the groove. The tendency was greatest in the wider groove (Hashimoto, 2021a). The two-dimensional area change of the cell relates not only to the deformation of the cell but also to the three-dimensional rotation of the cell, of which the shape deviated from a sphere.

In the present study, cells are sparsely suspended in the medium flow to reduce the interaction between cells. Cells can be sorted by the velocity change at the micro groove according to the diameter and the width of the groove. The expanded version of this study was presented at the IMECE conference in November 2021 (Hashimoto, 2021b).

5. Conclusions

The micro flow-channel with oblique micro grooves has been manufactured by the micromachining technique. The mechanism of the change in movement of the flowing cell over the oblique micro groove has been

analyzed. The result for each cell as it passes of a groove depends on the direction change of the major axis of the cell, which relates to the shape of the cell and the width of the groove.

6. Acknowledgments

The authors thank Mr. Akira Hayasaka and Mr. Shono Kuwabara for the help of the experiment.

References

Carlsen, P. N. (2020). *Polydimethylsiloxane: Structure and Applications*, Nova Science Publishers, 29-94.

Hashimoto, S., Takahashi, Y., Hino, H., Nomoto, R., & Yasuda, T. (2014). Micro Hole for Trapping Flowing Cell. *Proc. 18th World Multi-Conference on Systemics Cybernetics and Informatics, 2*, 114-119.

Hashimoto, S., Hayasaka, A., & Endo, Y. (2019). Sorting of Cells with Flow Channel: Movement of Flowing Myoblast Cell at Oblique Micro Grooves. *Proc. 23rd World Multi-Conference on Systemics Cybernetics and Informatics, 4*, 82-87.

Hashimoto, S., Matsuzawa, R, & Endo, Y. (2020). Analysis of Dielectrophoretic Movement of Floating Myoblast near Surface Electrodes in Flow Channel. *Proc. 11th International Multi-Conference on Complexity Informatics and Cybernetics, 2*, 13-18.

Hashimoto, S., Kuwabara, S., Yonezawa, H., & Endo, Y. (2021a). Effect of Shape of Cell on Movement over Micro Groove in Flow Channel. *Proc. 12th International Multi-Conference on Complexity Informatics and Cybernetics, 2*, 19-24.

Hashimoto, S., Yonezawa H., & Uehara, S. (2021b). Behavior of Cell Flowing Over Oblique Micro Rectangular Groove. *Proc. ASME 2021 International Mechanical Engineering Congress and Exposition*, IMECE2021-69696, 1-6.

LaBelle, C. A., Massaro, A., Cortés-Llanos, B., Sims, C. E., & Allbritton, N. L. (2021). Image-Based Live Cell Sorting. *Trends in Biotechnology, 39(6)*, 613-623.

Mutafopulos, K., Spink, P., Lofstrom, C. D., Lu, P. J., Lu, H., Sharpe, J. C., Franke, T., & Weitz, D. A. (2019). Traveling Surface Acoustic Wave (TSAW) Microfluidic Fluorescence Activated Cell Sorter (μFACS). *Lab on a Chip, 2019(19)*, 2435-2443.

Sivaramakrishnan M., Kothandan, R., Govindarajan, D. K., Meganathan, Y., & Kandaswamy, K. (2020). Active Microfluidic Systems for Cell Sorting and Separation. *Current Opinion in Biomedical Engineering* (Edited by Truskey, G., Fu, J., Verma, R. S., Ramakrishna, S.), *13*, 60-68.

Takahashi, Y., Hashimoto, S., Hino, H., Mizoi, A. & Noguchi, N. (2015). Micro Groove for Trapping of Flowing Cell. *Journal of Systemics, Cybernetics and Informatics, 13(3)*, 1-8.

Takahashi, Y., Hashimoto, S., Hino, H., and Azuma, T. (2016). Design of Slit between Micro Cylindrical Pillars for Cell Sorting. *Journal of Systemics Cybernetics and Informatics, 14(6)*, 8-14.

Takahashi, Y., Hashimoto, S., Mizoi, A., & Hino, H., (2017). Deformation of Cell Passing through Micro Slit between Micro Ridges Fabricated by Photolithography Technique. *Journal of Systemics Cybernetics and Informatics, 15(3)*, 1-9.

Yoon, Y., Lee, J., Ra, M., Gwon, H., Lee, S., Kim, M. Y., Yoo, K. C., Sul, O., C. G., Kim, W. Y., Park, J. G., Lee, S. J., Lee, Y. Y., Choi, H. S., & Lee, S. B. (2019). Continuous Separation

of Circulating Tumor Cells from Whole Blood Using a Slanted Weir Microfluidic Device. *Cancers, 11(200),* 1-13.

Zhang, Z., Chien, W., Henry, E., Fedosov, D. A., & Gompper, G. (2019). Sharp-edged Geometric Obstacles in Microfluidics Promote Deformability-based Sorting of Cells. *Physical Review Fluids, 4(2),* 1-18.